Session 3P1
Recent Advances in Optical Trapping and Binding

Comparison of Methods for the Calculation of Radiation Pressure on Dielectric and Magnetic Particles

B. A. Kemp, **T. M. Grzegorczyk**, **and J. A. Kong**
Massachusetts Institute of Technology, USA

The Maxwell stress tensor [1] and distributed Lorentz force [2, 3] are applied to calculate the time-average radiation pressure on two-dimensional (2D) dielectric and magnetic particles due to incident plane waves. We show that the two methods give identical results for the total force on a lossless medium. We use the Mie theory to calculate the fields scattered from an infinite circular cylinder used to represent a 2D particle, hence there is no restriction on the size of the particle considered. The results are verified using full-wave simulation results from the commercial software CST Microwave Studio ®.

The momentum conservation theorem is derived from the Lorentz force law where the charges and currents are represented by field quantities via the Maxwell equations. Using the momentum conservation theorem, the force on a lossless material body is described by the divergence of the Maxwell stress tensor and is calculated by the integration of the stress tensor on any surface which completely encloses the material body. Thus, the radiation pressure on a three dimensional (3D) object is calculated from a surface integral with knowledge of the total fields external to the object.

The distributed Lorentz force is applied to bound currents due to the polarization of a medium and to bound charges at the material boundary due to discontinuous $\hat{n} \cdot \epsilon_0 \bar{E}$ and $\hat{n} \cdot \mu_0 \bar{H}$, where $\hat{n}$ is the surface normal unit vector and ϵ_0 and μ_0 are the background permittivity and permeability. Contributions from magnetic current densities throughout a material body and magnetic charge densities at the surface are added to the standard Lorentz force on bound electric currents and charges to model the volume force density and the surface force density, respectively. The radiation pressure on a 3D object is determined by the combination of a volume integral with knowledge of fields and polarization inside the medium and a surface integral with contributions from fields on both sides of the boundary.

The results of the force calculation on 2D circular particles demonstrate that the two methods give equivalent results. The distributed Lorentz force can be applied to obtain the force density distribution throughout the medium, whereas the Maxwell stress tensor only provides the total bulk force on the particle. However, the Maxwell stress tensor reduces the surface integral to a line integral for the force on a 2D particle. Since the choice of force calculation method is independent of field calculation, either method can be extended to include multiple particles through the Foldy-Lax multiple scattering equations and to more complex geometries via numerical simulation. These computational abilities allow us to model the optical binding forces of multiple particles submitted to multiple incidences.

REFERENCES

1. Kong, J. A., *Electromagnetic Wave Theory* (EMW, 2000), ISBN 0-9668143-9-8, 2000.
2. Mansuripur, M., "Radiation pressure and the linear momentum of the electromagnetic field," *Optice Express*, Vol. 12, 5375–5401, 2004.
3. Zakharian, A. R., M. Mansuripur, and J. V. Moloney, "Radiation pressure and the distribution of electromagnetic force in a dielectric media," *Optics Express*, Vol. 13, 2321–2336, 2005.

Optical Binding of Small Particles

J. Ng[1], **Z. F. Lin**[1,2], **P. Sheng**[1], **and C. T. Chan**[1]

[1]The Hong Kong University of Science and Technology, China
[2]Fudan University, China

Light-trapping is generally associated with the phenomenon that small particles are driven toward the intensity maxima of a carefully sculpted laser beam. We show, through rigorous calculations, that in addition to the intensity-driven light-trapping due to gradient forces, a long-ranged optical binding force that can also induce stability in a cluster of small particles, even when the incident intensity is homogeneous. Under intense laser illumination (e.g., $10^6\,\mathrm{W/cm^2}$), such optical binding force can dominate over other interactions and bind dielectric microspheres into stable structures that behave like "molecules" which has well defined geometries and vibrational modes. Such photonic clusters can exhibit a multiplicity of static and drifting equilibrium configurations, with some having remarkable geometries such as a quasicrystal-like arrangement. Owing to the nonconservative nature of the system, the photonic clusters exhibit exotic dynamics, and the equilibrium configurations can correspond with either stable or a type of quasi-stable states in which the cluster maintains an average shape, with individual particles executing periodic motion in the presence of frictional dissipation. Photonic clusters consist of Rayleigh particles are also investigated. In contrast to microparticle-cluster which exhibits nonconservative dynamics, the interaction of Rayleigh particles is essentially conservative when the incident wave is a standing wave.

We also consider the light-induced stability of extended system and an interesting stable one-dimensional lattice is found and analyzed. Through analyzing its characteristic vibration modes, we observe, in addition to phonon-like lattice vibrations which are spatially extended, spatially localized modes. The localized modes can be attributed to the extraordinarily long-ranged optical binding force and the underlining principle suggests that similar type of mode is expected for other optically structure that are extended in size.

We also consider another type of inter-particle optical force that is driven by resonance. We found that the tuning of the incident light's frequency to the morphology-dependent resonances of a cluster of high-Q microspheres induces a strong, resonant optical force between the spheres. In contrast to the long range optical binding force described previous, this resonant optical force is very short ranged. The resonant force can be enhanced by orders of magnitude so that it dominates other interactions at modest incident intensity (e.g., $10^4\,\mathrm{W/cm^2}$).

Advanced Studies in Optical Binding

K. Dholakia[1,2], **N. K. Metzger**[1], **and E. M. Wright**[2,1]

[1]University of St Andrews, UK
[2]The University of Arizona, USA

Optical forces arise due to the light matter interaction. These forces have had impact right from the single atom level through Bose-Einstein condensates up to biological cells and colloidal matter. Light-matter interactions may be used to dictate the organization and manipulation of colloidal and biological matter at the microscopic level. An inhomogeneous optical field permits dielectric spheres of higher refractive index than their surrounding medium to be trapped in three dimensions in the field maxima primarily through the dipole interaction [1]. This allows physicists, chemists and biologists to explore a range of fundamental phenomena. From a physics perspective this includes thermally activated escape from a potential well, studies of optical angular momentum, stochastic resonance and various studies of colloidal behaviour in external potentials. From a biological perspective optical trapping has revolutionised our understanding of molecular motors.

Non-zero order light patterns and various families of propagating light fields are of significant interest across numerous branches of the sciences. If one goes beyond a standard Gaussian beam one may look at examples such as Hermite-Gaussian, Laguerre-Gaussian and Bessel light modes. These latter two modes possess cylindrical symmetry and have been of interest for studies of optical angular momentum, optical vortices, micromanipulation and for novel beam characteristics (e.g., studies of the Poynting vector and their reconstruction). Other extended two and three dimensional light patterns too have become of widespread interest: in the realm of optical micromanipulation they may create extended potential energy landscapes that may allow novel studies of extended colloidal systems and interactions therein.

Deformation of the light pattern by the very interaction of the particle with the imposed light field is a relevant issue for three dimensional structures which might be created using these techniques. The light matter interaction may lead to "optical binding". Such "optical binding" is radically different from conventional predefined trapping alluded to above: Here the very interaction between an object and its nearest neighbors creates a self consistent and homogeneous solution that allows an optical geometry to, in principle, create a large scale colloidal array. This topic has come again to the fore: work over a decade ago shows this effect in studies of Burns, Golovechenko and Fournier [2]. The St Andrews group have looked at new forms of optical binding in both counter-propagating and vertical geometries [3]. The key is that the interparticle spacing here is, unlike the earlier form of optical binding, of the order of microns and indeed the stronger interaction between the particles is key to creating the new forms of bound matter currently under study in our group. Interesting behaviour such as bistability may be observed.

In this talk I will discuss recent work on optical trapping in extended light patterns and primarily concentrate on the latest data in the area of optical binding which is proving a rich and surprising area in this field.

REFERENCES

1. Neuman, K. and S. Block, *Rev. Sci. Instrum.*, Vol. 758, 2787, 2004, D. Grier, *Nature*, Vol. 424, 810, 2003; K. Dholakia, G. Spalding, and M. MacDonald, *Physics World*, Vol. 15, 31, Oct. 2002.
2. Burns, M. M., J.-M. Fournier, and J. A. Golovchenko, *Phys. Rev. Lett.*, Vol. 63, 1233, 1989; M. M. Burns, J.-M. Fournier, and J. A. Golovchenko, *Science*, Vol. 249, 749, 1990.
3. Tatarkova, S. A., A. E. Carruthers, and K. Dholakia, *Phys. Rev. Lett.*, Vol. 89, 283901, 2002; D. McGloin, A. E. Carruthers, K. Dholakia, and E. M. Wright, *Phys. Rev. E*, Vol. 69, 021403, 2004; V. Garcés-Chávez, D. Roskey, M. D. Summers, H. Melville, D. McGloin, E. M. Wright, and K. Dholakia, *Appl. Phys. Lett.*, Vol. 85, 4001, 2004.

Simulating the Optical Force and Torque on Metallic Nano-particles

C. Rockstuhl
Friedrich Schiller University Jena, Germany

In this paper we analyze force and torque induced by optical fields on single and coupled silver nano-particles as a function of the wavelength. The geometry of the nano-particles is either a cylindrical one with circular or elliptical cross section or a spherical one.

The most prominent property of those metallic nano-particles is the excitation of the small particle surface plasmon polaritons at well-defined wavelength for which the dielectric constant of the materials takes appropriate values. The resonant oscillation of the free electrons with the frequency of the illuminating wave field causes a tremendous enhancement of the near-field amplitude and the scattering cross section. Such an enhanced scattering might find application in a modified version of a scattering type scanning near-field optical microscope, in which a nano-particle trapped by an optical beam is scanned shortly above the surface of a sample or in a photonic force microscope [1].

For trapping such a particle, all forces acting on it have to be equilibrated. The main forces are the scattering and the gradient force, whereby the first one is proportional to the intensity and the square of the polarizability and it points towards the propagation direction of the laser beam, whereas the latter one is proportional to the gradient of the intensity and the polarizability. If the gradient force is sufficiently strong for compensating the scattering force, the particle is trapped in a position shortly after the waist of a laser beam that has a Gaussian amplitude distribution in the transversal coordinate. For spatial positions deviating from that equilibrium position, the particle is linearly accelerated due to a non-zero net force. In addition to that linear acceleration, non-spherical particles are rotationally accelerated due to a torque and they will align themselves within the wave-field.

In this paper we use the Multiple Mulitipole Method [2] and Mie Theory [3] for a rigorous computation of the wavelength dependent force and torque acting on metallic nano-particles. The observed behavior is physically explained using arguments based on the dipole approximation. It will be shown that different interaction regimes with respect to the plasmon wavelength of the particle exist and specific behavior appears in the different regimes due to a different sign of the polarizability. The conditions for a stable trapping of the particles will be elucidated and the stability of the particles is estimated by comparing the optical force with the Brownian force.

REFERENCES

1. Rohrbach, A., E. L. Florin, and E. H. K. Stelzer, "Photonic force microscopy: simulation of principles and applications," *Proc. SPIE*, Vol. 4431, 75, 2001.
2. Hafner, C., "Post-Modern electromagnetics," *John Wihley & Sons*, 1999.
3. Barton, J. P., D. R. Alexander, and S. A. Schaub, "Theoretical determination of net radiation force and torque for a spherical particle illuminated by a focused laser beam," *J. Appl. Phys.*, Vol. 66, 4594, 1989.

Trapping of Microscopic Particles in Specially Designed Optical Fields

S. Bernet and M. Ritsch-Marte
Medical University of Innsbruck, Austria

We report and discuss a few milestones — and side-tracks — reached on our way to ever increasing control over the manipulation of microscopic objects.

Fiber-optical traps, for instance, are ideally suited to investigate the subtle interplay between the light field and the particle positions, which spontaneously leads to a *self-organized* linear array of trapped particles with a spacing which is mainly determined by the particle size. A self-consistent model, valid for particle sizes below the wavelength, was able to predict our experimental findings very well.

If one seeks to predefine the trapping arrangement rather than deal with a self-organized pattern, one may use holographic optical tweezers to create complex light distributions for optical micromanipulation. We show how holographically projected images can be optimized using a setup in the Fresnel regime (intermediate field) instead of the typically used Fourier regime (far-field). Special laser modes like Laguerre-Gaussian beams (doughnut modes) or arbitrary superpositions of such modes can be generated with a high purity, with appealing effects on trapped particles: For example, the size of optical tweezers created by a doughnut mode can be utilized for size-selective trapping of micro-particles.

One may also use static light fields for producing a continuous flow of micro-particles, e.g., an all-optical micro-pump which is driven by orbital angular momentum transfer from the laser modes to the particles. Such optical micro-devices can be locally integrated in an active or passive particle sorting system wherever one needs to generate a flow.

Tailored arrangements of these functional optical fields may be used to create automated microscopic tools for the assembly of microstructures, for the sorting of biological samples, or for the manipulation of selected components within intact biological samples. We report our recent developments approaching these goals.

Polarization Effects in Optically Bound Particle Arrays

C. D. Mellor
University of Oxford, UK

C. D. Bain
Durham University, UK

We have recently reported the formation of optically bound arrays of sub-micron polystyrene particles in the evanescent wave of two counterpropagating laser beams incident at the silica-water interface above the critical angle for total internal reflection([1, 2]). In this talk, we will describe some of the effects of the polarisation of the incident lasers on the packing of the arrays. Under the experimental conditions, the amplitude of the incident field is nearly identical for the two polarisations, but the field is in the surface plane for s-polarised light and almost perpendicular to the surface plane for p-polarised light. The case of orthogonally polarised laser beams has also been explored.

A number of different packing motifs are observed, including centred rectangular and several types of pseudohexagonal arrays that are distinguished by their orientation and periodicity of the lattice. With p-polarised light we have also observed missing row structures, such as that shown in the figure below, in which every third interference fringe is unoccupied. The fringe separation (400 nm) is indicated; the particle diameter is 520 nm. A variety of packing defects are observed, including lattice vacancies and twin planes (such as that shown with an arrow in the figure below). Defects heal at different rates for different polarisations. More than one form of packing can sometimes be observed under the same polarisation conditions, suggesting the presence of multiple minima in the many-body potential energy surface.

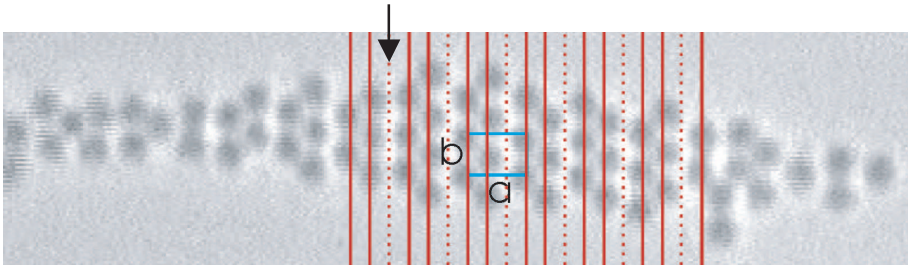

REFERENCES

1. Mellor, C. D. and C. D. Bain, *Optical Trapping and Optical Micromanipulation II.*
2. Dholakia, K. and G. C. Spalding, *Proc. SPIE*, Vol. 5930, 352, Eds., 2005.

Optical Binding in Air

M. Guillon
Laboratoire d'Interférométrie Stellaire et Exoplanétaire, France

Abstract—Optical binding between micron-sized oil droplets in air has recently been observed. The experimental setup, consisting in two vertical, counter propagating and diverging laser beams, builds up a three dimensional trap. The cloud of oil droplets, enclosed in a glass cell, progressively fills in the trap where droplets interact one with another. Scattered intensity is observed on a video camera. Interactions involve optical, electrostatic, radiometric and capillary forces. Orders of magnitude are discussed.

Chains up to four droplets have been observed, the most stable structure being the doublet and not the single drop. In air, viscosity being one thousand times smaller than in water, mean free path of a micro-sphere is much bigger. That is why mean residence times in metastable states are of the magnitude of a few seconds and that brownian motion quickly drives the trapped droplets in the very minimum of potential energy: the doublet structure. Two stable states have also been obtained for the doublet. Observation of interference indicates that oil droplets are phase-locked onto each other every $\lambda/2$.

The spraying technique we use, gives droplets smaller than the micron in radius. This is the intermediate case of the Mie range between the small and large wavelength cases. Those new experimental results exhibit the role of the short and long range interactions in optical binding. They are then theoretically discussed both in the ray model and in the Rayleigh approximation, and compared with previous works on optical binding in water. Moreover, in our case, the index contrast is much bigger. It implies stronger scattered intensities, bigger interaction forces with light and therefore, bigger binding forces.

1. Introduction

Since the pioneering work by Ashkin [1] in the early 1970's, optical tweezers have nowadays become a commonly used tool for micromanipulation in water. Optical trapping in air and vacuum remains a difficult task due to Van der Waals forces several orders of magnitude larger than optical forces. In the literature, two possibilities were explored: the use of aerosols[1–4] and mechanical vibration coupled with strongly focused cw laser beams [5, 16, 7, 8]. Afterwards, self-assembled structures of microparticles under strong laser illumination have been demonstrated [9–12]. Optical binding was observed when the particle separation is either othogonal or along the light propagation. When the separation is set orthogonal to the beam propagation and to beam polarization, theory predicts potential minima every l for particles in the Rayleigh range [13]. This l periodicity was experimentally observed for polystyrene spheres in the Mie range in water [10]. The Mie correction to Rayleigh approximation was supposed to modify the interaction strength more than the periodicity. In three dimensional optical traps made with two counter-propagating beams, potential minima appeared to be along the beam axis. Due to the weakly focused beams and to gradient forces, the particles are constrained to remain on the beam axis. Optical interactions then lead to chains where spheres are either stuck or separated by more than a diameter away [12]. For spheres in the Rayleigh range, potential minima every $\lambda/2$ are expected.

Trapping in air imposes a tridimensional trap since the Van der Waals forces are not negligible as is the case in water. However, the larger index ratio gives larger cross sections and the optical forces are consequently stronger than in water.

2. Experiment

Our experiment [15] deals with micron-sized oil-droplets in air obtained with a spray nozzle. According to their falling time, their diameter was estimated to be in the range between 1 μm and 1.5 μm. They are protected from air convection currents by a glass cell. We use a 30 mW frequency doubled YAG laser at 532 nm. The optical trap consists in two weakly focused ($N.A. = 1/15$) and counter-propagating laser beams (see Fig. 1). The return beam is focused roughly $300\mu m$ before the forward beam. The equilibrium position of trapped particles is at half distance of both focusing points, where the intensities of the two beams are equal. The geometry is then similar to those previously studied in water [11, 12] with optical fibers. We chose a vertical geometry in order to oppose gravity with the scattering force rather than with the gradient force which is much weaker for spheres in the Mie range.

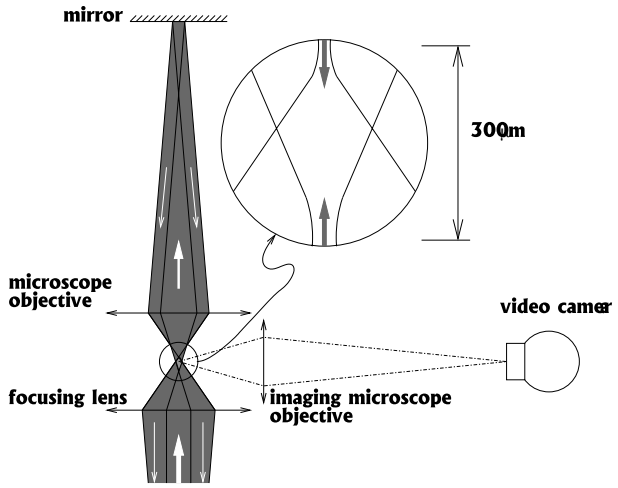

Figure 1: Experiment principle. The scattering force is opposed to gravity. The forward beam is retro-reflected on a mirror at the focus of a lens. The downward returning beam is focused 300 μm above the upward direct beam so as to build a stable equilibrium zone. The laterally scattered intensity is observed on a video camera through a 10x, 0.25NA microscope lens. A cell of glass, not shown, protects from air motion.

3. Results

3.1. Trapped Structures

When the cell is filled with an oil droplet cloud, radiation pressure pushes the droplets inside the trap. By far, the most common structure observed was a doublet. We rarely saw a single droplet. Three and four droplet chains were also seen for a few seconds before changing into a doublet by escaping or merging processes. Coallescence with outer droplets—tends to increase progressively the size of both droplets in a doublet. The increasing finishes when the cloud of droplet has fallen down. We observed that in a doublet, the larger the droplets, the further apart. We never saw a doublet collapsing or splitting away. The optical binding forces in this case, appears to be much stronger than all other forces.

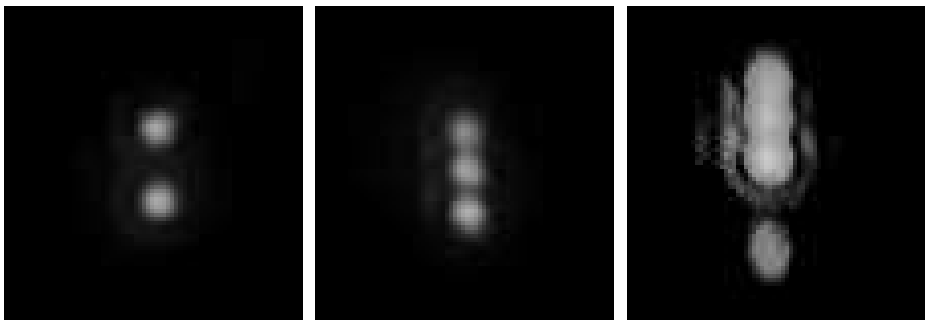

Figure 2: Doublet, triplet and quadruplet structures. The doublet is observed to be the most stable structure is the doublet. Its droplets are spaced approximately 3.5 μm apart, between centers. The length scale is the same for all the pictures.

On a few occasions, we observed a sudden change of the doublet's appearance, mainly regarding the interference of both Airy patterns on the camera. On the first picture (see Fig. 3), images of droplets interfere such as to give a dark fringe between droplets while on the second picture, we see bright dots on the symmetry axis. In the first case, droplets are scattering in phase opposition as in the second case, they are emitting in phase, corresponding to a $\lambda/2$ difference of distance. An estimate of the difference of distance separations of doublets gave values close to $\lambda/2$. This measurement is difficult due to the low resolution power of the imaging microscope objective. This phenomenon was assumed to be a swiching between two stable states of a doublet, which can be understood in the dipolar approximation as explained further.

Figure 3: Two different equilibrium states of a 2.3 μm doublet. The main difference is the interference pattern. On the first picture, droplets are emitting in phase opposition, we see a dark fringe on the symmetry axis. On the second one, they are emitting in phase, bright dots can be seen on the symmetry axis. It suggests that the difference of separation distance between droplets increased. We estimated the increasing to be of the order of half a wavelength in accordance with the interference pattern.

3.2. Clinging to Fringes

When trapped, particles move quikly due to speckle. Static speckle is introduced with dirtyness of optical components. Dynamic speckle is also introduced by the cloud of droplets crossing the trapping beams. Disturbance caused by the cloud is larger when a droplet cross the beam in the vicinity of the focusing point.

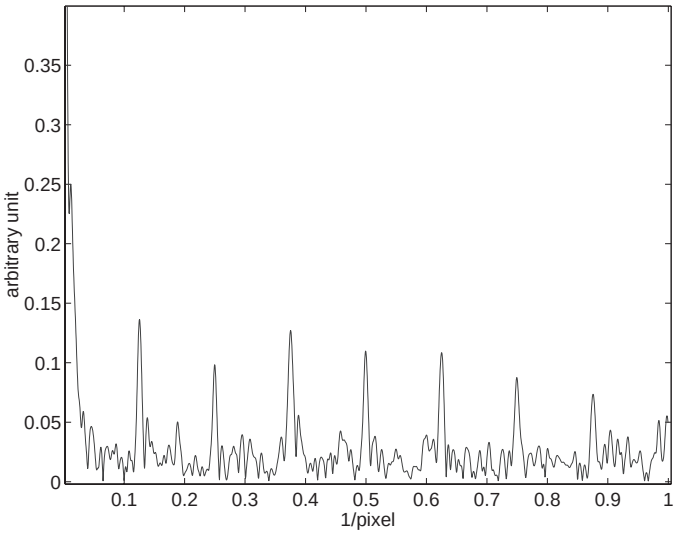

Figure 4: Position spectrum of the doublet in the trap.

The laser we use has two longitudinal modes. There are coherence beatings every three millimeters. After a 30 cm optical path, we do not know if the return beam is coherent with the upward one. In the case where the two counter-propagating beams are coherent, a stable $\lambda/2$ fringe pattern should trap the structure. If the brightness contrast is not large enough, the gradient force is weak and small intensity fluctuations between the two counter propagating beams can unbalance the well's minimum in the longitudinal direction. In this case, the doublet quickly (compared with the frame rate of the video camera) sweeps a sinusoidal potential well. As images of droplets are several pixels wide, their positions can be measured with a subpixel resolution. We performed the Fourier transform of the positions y_p of the doublet in the trap when counter-propagating beams were circularly polarized and weakly coherent (see Fig. 4):

$$\mathcal{F}(Y)(\sigma) = \sum_p e^{2\pi i \sigma y_p}$$

The same numerical calculation for the case of a crossed-polarized beams experiment does not give those peaks. According to imaging power $\lambda/2 \simeq 1.6 pixel$, the main harmonic is then the 0.62 peak. The other peaks are folded back harmonics. We can see that they are numerous and Dirac comb like, which means that the doublet very likely mechanically clings to fringes and the position spectrum we obtain cannot be a light modulation measurement artefact.

3.3. Theoretical Discussion on Binding

In our experiment, the spheres radii are from 0.5 μm up to 1.2 μm when several droplets have merged. Those values correspond to ka (a being its radius and k the wave vector) between 12 and 14. For particles in the Mie regime which is the case, numerical calculations have to be performed and multiscattering processes must be taken into account to know the exact optical binding forces [14]. However, in this regime, the particles' behaviour looks like both dipoles and large spheres. In this discussion, we aim at giving a flavour of the physics of the binding effect. We think this experiment can be approximately understood from the two extreme regimes of the ray model and the Rayleigh range.

When spheres are such that $ka < 1$ or when $kr > 1$ (r being the separation distance between spheres), the dipole approximation is sufficient to estimate potential minima. In this approximation, optical interactions between particles are maximal when the separation is orthogonal to polarization. It can be either along or transverse to the beam axis. In agreement with dipolar theory, it was experimentally observed [10] that potential wells for two particles were every λ, the wavelength. When the separation is along the wave vector, a similar calculation predicts potential wells roughly every $\lambda/2$:

$$V = -\left|\frac{\cos\varphi + f(kr)e^{ikr}\cos(kr+\varphi)}{1 - f(kr)^2 e^{2ikr}}\right|^2$$

with

$$f(kr) = k^3\alpha\left(\frac{1}{kr} - \frac{1}{(kr)^3} + \frac{i}{(kr)^2}\right)$$

$\alpha = \dfrac{n^2-1}{n^2+2}a^3$ being the polarizability of the (identical) dielectric spheres of index n, and r being the separation between the two spheres. The denominator corresponds to the Mossotti resonance in atom trapping. It can only be zero for resonant particles for which the real part of f can be larger than one. This can never happen with dielectric or even metallic particles: the spheres touch before the resonance happens. When $kr > 1$, we can approximate the previous formula by:

$$V \simeq -\cos\varphi\left(\cos\varphi\left(1 + \frac{k^3\alpha}{kr}\right) + \frac{k^3\alpha}{kr}\cos(2kr+\varphi)\right)$$

which exhibit a $\lambda/2$ periodicity which is consistent with the experimental observation (Fig. 3).

However we could not see jumps between many $\lambda/2$-separated potential wells like in Fournier's experiment [10]. The two droplets remain at a quite stable distance depending on their size. This comportement looks like that of large spheres.

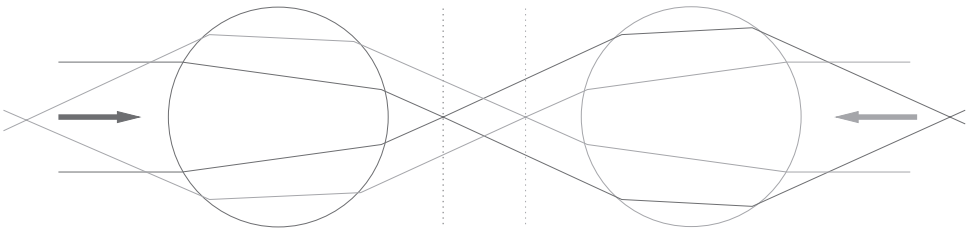

Figure 5: Principle of binding between two spheres in the ray model. Each droplet acts as a tweezer for the other. As there is no reason why focal plans of spheres be the same, the second sphere defocuses its trapping tweezer and can rebuild another tweezer behind it like in triplet cases or 4-droplet cases.

When the radius of spheres is such that $ka > 100$, optical forces can be calculated in the ray model approximation with a good degree of accuracy [6, 17]. In this model, binding between two spherical dielectric particles can be understood by comparison with optical tweezers. For a sufficiently focused beam, a dielectric particle can be trapped close to the focal point. In our case, the focusing lens is nothing else than the next droplet. Each droplet builds an optical tweezer for the other. The numerical aperture of a spherical lens can be approximated by $NA \simeq \dfrac{a}{f} = 2\dfrac{n-1}{n}$ which only depends on the index of the sphere (not on its radius). We think this model explains the high stability of the doublet structure despite speckle: a single plane seems to be sufficient for particles to be bound. For reaching such stability, spheres need to be close enough to each other.

When spheres are much more than a diameter away like in the case of experiments in water [11, 12], spheres cannot be in a bound state: the focusing numerical aperture is not sufficient for the optical tweezer to be stable. In this case, microspheres interact repulsively in a single trap so as to give chains. This comparison with optical tweezers can also explain why structures with three and four droplets are less stable than the doublet case. Indeed, while being trapped by the tweezer, the sphere defocuses the beam (see Fig. 5). However, there is no reason why the optical force be zero when the focal point of the first droplet is the same as the focal point of the second. We can then hope, for a given radius of sphere (even more in the Mie range) a configuration where the second sphere will be trapped at two focal lengths of the focusing point. In this case, neglecting spherical aberrations, the second sphere will rebuild a trap behind it. This argument explains both the possibility to build 4-droplet chains and why the doublet is much more stable than triplets and quadruplets.

3.4. Orders of Magnitude

We can see on movies than despite all the disturbing sources, the doublet is very stable, even when the laser beam is cut for one second. We present here the main forces involved in this experiment.

The strongest forces are capillary forces. For particles smaller than $1.2\,\mu$m in radius, they can be estimated with Laplace's theorem: $\Delta P = \dfrac{2\gamma}{a} \simeq 10^5\,\mathrm{pN}.\mu\mathrm{m}^{-2}$ where ΔP is the pressure difference between inside and outside the droplet, γ is the capillary coefficient of the liquid and a the radius of the sphere. This pressure must be compared with the electromagnetic pressure of the order of I/c. In a binding case, field can be enhanced between particles so as to increase the optical force by one order of magnitude. However, if we simply consider the trapping pressure, we obtain in the case of our experiment a pressure equal to $1\,\mathrm{pN}.\mu\mathrm{m}^{-2}$.

Brownian motion could also destruct the phase locking observed between bound droplets. As the interference pattern between images of droplets of a doublet remains despite random forces, we can conclude that the distance never changes more than $\lambda/4$. It means that the mean thermal force over a distance $\lambda/4$ is smaller than $\dfrac{kT}{\lambda/4} \simeq 10^{-2}\,\mathrm{pN}$. To be compared with the pressures we calculated in the previous paragraph, we can approximate the radius of spheres to be one micron. Finaly, as droplets are negatively charged when sprayed due to triboelectricity effects with the spray nozzle, electrostatic forces causes droplet repealing. Each droplet carry a few elementary charges and the distance between droplets being roughly $2.5\,\mu$m: $F = \dfrac{1}{4\pi\epsilon_0}\dfrac{qq'}{r^2} \simeq 10^{-5}\,\mathrm{pN}$. Electrostatic forces are then three orders of magnitude smaller than optical forces.

We should add an estimate of heating effects. As oil slightly absorbs light, convection currents may appear inside droplets. This effect has already been discussed in a previous article [15] but a precise idea of the forces involved cannot be given.

4. Conclusion

Our experimental results obtained in air differ appreciably from those previously reported in water. Much of the difference probably results from the higher index contrast. Our results fit both with a Rayleigh range binding process and a semi-classical ray model.

Acknowledgment

I would like to thank particularly Professor A. Labeyrie for fruitful advice and support, and acknowledge Professor J.-M. Fournier for his helpful encouragement.

REFERENCES

1. Ashkin, A., *Phys. Rev. Lett.*, Vol. 24, 156–159, 1970.
2. Ashkin, A. and J. M. Dziedzic, *Appl. Phys. Lett.*, Vol. 28, No. 6, 333–335, 1975.
3. Magome, N., M. I. Kohira, E. Hayata, S. Mukai, and K. Yoshikawa, *J. Phys. Chem. B*, Vol. 107, 3988–3990, 2003.
4. Hopkins, R. J., L. Mitchem, A. D. Ward, and J. P. Reid, *Phys. Chem. Chem. Phys.*, Vol. 6, 4924–4927, 2004.
5. Ashkin, A. and J. M. Dziedzic, *Appl. Phys. Lett.*, Vol. 19, No. 8, 283–285, 1971.
6. Pocholle, J.-P., J. Raffy, Y. Combemale, M. Papuchon, G. Roosen, and M. T. Plantegenest, *Appl. Phys. Lett.*, Vol. 45, No. 4, 350–352, 1984.
7. Omori, R., T. Kobayashi, and A. Suzuki, *Opt. Lett.*, Vol. 22, No. 11, 816–818, 1997.

8. Omori, R., K. Shima, and A. Suzuki, *Jpn. J. Appl. Phys.*, Vol. 38, L743–L745, 1999.
9. Burns, M., J.-M. Fournier, and J. A. Golovchenko, *Science*, Vol. 249, 749–754, 1990.
10. Burns, M., J.-M. Fournier, and J. A. Golovchenko, *Phys. Rev. Lett.*, Vol. 63, No. 12, 1233–1236, 1989.
11. Tatarkova, S. A., A. E. Carruthers, and K. Dholakia, *Phys. Rev. Lett.*, Vol. 89, 283901,1–4, 2002.
12. Singer, W., M. Frick, S. Bernet, and M. Ritsch-Marte, *J. Opt. Soc. Am. B*, Vol. 20, No. 7, 1568–1574, 2003.
13. Depasse, F. and J.-M. Vigoureux, *J. Phys. D: Appl. Phys.*, Vol. 27, 914–919, 1993.
14. Moine, O. and B. Stout, *J. Opt. Soc. Am. B*, Vol. 22, 8, 2005.
15. Guillon, M., *SPIE Proceedings*, 5930–62, 2005.
16. Roosen, G., *C. Imbert, Phys. Lett.*, Vol. 59A, 6, 1976.
17. Gussgard, R., T. Lindmo, and I. Brevik, *J. Opt. Soc. Am.* Vol. B, No. 9, 10, 1991.

Optical Waveguide Manipulation of Micro- and Nano-spheres

J. S. Wilkinson[1], **O. G. Hellesø**[2], **J. P. Hole**[1], **and K. Grujic**[2]

[1]University of Southampton, UK
[2]University of Tromsø, Norway

Optical tweezers are well-established as a tool for non-contact, non-destructive handling of biological materials [1] and of inorganic nanospheres attached to biological molecules [2]. Recently, interest has grown in optical manipulation at surfaces [3] potentially as part of the toolbox of the "lab-on-a-chip". In particular, advances have been made in trapping and propulsion of metallic and dielectric micro- and nano-particles in the evanescent fields of optical waveguides [4, 5], which may form part of a planar microsystem into which optical detection and spectroscopy of separated species could also be integrated. Optical waveguides embedded in surfaces represent a powerful means of controlling the distribution of optical intensity and intensity gradient at such surfaces, for particle control.

In this paper, the design of optical waveguides and waveguide devices for trapping, propulsion and sorting of gold nanospheres and latex microspheres [6, 7] will be described and recent experimental results presented and compared with theoretical models. The implications of these results for some proposed applications in the biosciences will be discussed.

REFERENCES

1. Ashkin, A., J. M. Dziedic, and T. Yamane, "Optical trapping and manipulation of single cells using infrared laser beams," *Nature*, Vol. 330, 769, 1987.
2. Arai, Y., R. Yasuda, K. Akashi, Y. Harada, H. Miyata, K. Kinosita, and H. Itoh, "Tying a molecular knot with optical tweezers," *Nature*, Vol. 399, 446, 1999.
3. Kawata, S. and T. Sugiura, "Movement of micrometer-sized particles in the evanescent field of a laser beam," *Optics Letters*, Vol. 17, 772, 1992.
4. Kawata, S. and T. Tani, "Optically driven mie particles in an evanescent field along a channeled waveguide," *Optics Letters*, Vol. 211, 768, 1996.
5. Ng, L. N., M. N. Zervas, J. S. Wilkinson, and B. J. Luff, "Manipulation of colloidal gold nanoparticles in the evanescent field of a channel waveguide," *Applied Physics Letters*, Vol. 76, 1993, 2000.
6. Grujic, K., O. G. Hellesø, J. P. Hole, and J. S. Wilkinson, "Sorting of polystyrene microspheres using a Y-branched optical waveguide," *Optics Express*, Vol. 13, 1, 2005.
7. Hole, J. P., J. S. Wilkinson, K. Grujic, and O. G. Hellesø, "Velocity distribution of gold nanoparticles trapped on an optical waveguide," *Optics Express*, Vol. 13, 3896, 2005.

Towards Efficient Modelling of Optical Micromanipulation of Complex Structures

T. A. Nieminen, V. L. Y. Loke, A. M. Brańczyk
N. R. Heckenberg, and H. Rubinsztein-Dunlop
The University of Queensland, Australia

Abstract—Computational methods for electromagnetic and light scattering can be used for the calculation of optical forces and torques. Since typical particles that are optically trapped or manipulated are on the order of the wavelength in size, approximate methods such as geometric optics or Rayleigh scattering are inapplicable, and solution or either the Maxwell equations or the vector Helmholtz equation must be resorted to. Traditionally, such solutions were only feasible for the simplest geometries; modern computational power enable the rapid solution of more general — but still simple — geometries such as axisymmetric, homogeneous, and isotropic scatterers. However, optically-driven micromachines necessarily require more complex geometries, and their computational modelling thus remains in the realm of challenging computational problems. We review our progress towards efficient computational modelling of optical tweezers and micromanipulation, including the trapping and manipulation of complex structures such as optical micromachines. In particular, we consider the exploitation of symmetry in the modelling of such devices.

1. Introduction

Optical tweezers have seen deployment in a wide range of applications in biology, soft materials, microassembly, and other fields. As well as being used for the trapping and manipulation of a wide range of natural and artificial objects, optically trapped probes are used to measure forces on the order of piconewtons. Compared with this diverse range of experimental applications, theory and accurate computational modelling of optical tweezers has received much less attention and has remained relatively undeveloped, especially for non-spherical particles and non-Gaussian beams. This is unfortunate, especially when we consider the growing fields of controlled rotation of complex microparticles — prototype optically-driven micromachines — and fully three-dimensional manipulation using complex optical fields, where the application of theory and modelling provide insight into the physics, and allow engineering and optimisation.

Since optical forces and torques result from the transfer of momentum and angular momentum from the trapping beam to the particle via scattering, the theory and computational modelling of optical tweezers is, in essence, the theory and computational modelling of the scattering of light or electromagnetic radiation. Since typical particles that are optically trapped or manipulated are on the order of the wavelength in size, approximate methods such as geometric optics or Rayleigh scattering are inapplicable, and solution or either the Maxwell equations or the vector Helmholtz equation must be resorted to. As scattering by particles in this size range is of interest in many fields, a wide variety of analytical and computational methods have been developed. Thus, there is a solid foundation on which to develop computational modelling of optical micromanipulation.

There are, however, complications that prevent simple direct application of typical light-scattering codes. The first, but not necessarily the most important, is that optical tweezers makes use of a highly focussed laser beam, while most existing scattering codes assume plane wave illumination. Perhaps more fundamental is the need for a large number of repeated calculations to characterise an optical trap — even for an axisymmetric (but nonspherical) particle trapped in a circularly polarised Gaussian beam, we already have four degrees of freedom. Clearly, this places strong demands on computational efficiency.

Due to this requirement for repeated calculation of scattering by the same particle, we employ the T-matrix method [1, 2]. Below, we outline the employment of the T-matrix method for the calculation of optical forces and torques. While most implementations of the T-matrix method are restricted to simple geometries, this is not a limitation inherent in the method; fundamentally, the T-matrix method is a *description* of the scattering properties of a particle, not a method of calculating the scattering properties. Therefore, in principle, any method of calculating scattering can be used to obtain the T-matrix for a scatterer. We discuss such "hybrid" methods, where a computational method not usually associated with the T-matrix method is used to calculate the T-matrix of a scatterer, and hence the optical force and torque.

A further important consideration is that optical micromachines, while complex, are likely to possess a high degree of symmetry; this can be exploited to reduce computation times by orders of magnitude. We demonstrate

the effectiveness of this approach by modelling the optical trapping and rotation of a cube. The two principal symmetries of such shapes — mirror symmetry and discrete rotational symmetry about the normal to the mirror symmetry plane — are exactly the symmetries that typify the ideal optically-driven rotor.

2. *T*-matrix Formalism for Optical Force and Torque

The T-matrix method in wave scattering involves writing the relationship between the wave incident upon a scatterer, expanded in terms of a sufficiently complete basis set of functions $\psi_n^{(\mathrm{inc})}$, where n is a mode index labelling the functions, each of which is a solution of the Helmholtz equation,

$$U_{\mathrm{inc}} = \sum_n^{\infty} a_n \psi_n^{(\mathrm{inc})}, \tag{1}$$

where a_n are the expansion coefficients for the incident wave, and the scattered wave, also expanded in terms of a basis set $\psi_k^{(\mathrm{scat})}$,

$$U_{\mathrm{scat}} = \sum_k^{\infty} p_k \psi_k^{(\mathrm{scat})}, \tag{2}$$

where p_k are the expansion coefficients for the scattered wave, is written as a simple matrix equation

$$p_k = \sum_n^{\infty} T_{kn} a_n \tag{3}$$

or, in more concise notation,

$$\mathbf{P} = \mathbf{TA} \tag{4}$$

where T_{kn} are the elements of the T-matrix. The T-matrix formalism is a Hilbert basis description of scattering. The T-matrix depends only on the properties of the particle — its composition, size, shape, and orientation — and the wavelength, and is otherwise independent of the incident field.

This means that for any particular particle, the T-matrix only needs to be calculated once, and can then be used for repeated calculations. This is the key point that makes this an attractive method for modelling optical tweezers, providing a significant advantage over many other methods of calculating scattering where the entire calculation needs to be repeated.

The natural choice of basis functions when describing scattering by a compact particle is to use vector spherical wavefunctions (VSWFs) [1]. The optical force and torque are given by sums of products of the modal amplitudes [3–5].

Notably, neither how the VSWF expansion of the incident field nor how the T-matrix can be calculated has entered the above description of scattering. A variety of methods exist for the former [6, 5], and the latter task is generally the more challenging computationally.

Most implementations of the T-matrix method use the extended boundary condition method (EBCM), also called the null field method, to calculate the T-matrix. This is so widespread that the T-matrix method and the EBCM are sometimes considered to be inseparable, and the terms are sometimes used interchangeably. However, from the description above, it is clear that the T-matrix formalism is independent of the actual method used to calculate the T-matrix [7, 8].

A number of alternative methods have been used for the calculation of T-matrices. Notably, such "hybrid" methods, for example the discrete dipole approximation (DDA) method used by Mackowski [9] can be used for the calculation of T-matrices for particles of arbitrary shape, internal structure, and electromagnetic properties. Complex internal structure will generally require a discretisation of the internal volume of the particle, rather than a method based on surface discretisation. We are working on both finite-difference frequency-domain (FDFD) and DDA based hybrid T-matrix solvers.

3. Optical Torque and Symmetry

The T-matrix elements are strongly dependent on the symmetry of the scatterer [1]. We can deduce the principal features from Floquet's theorem, relating solutions to differential equations to the periodicity of their boundary conditions.

If we have a scatterer with nth-order rotational symmetry about the z-axis, an incident mode of azimuthal index m couples to scattered modes with azimuthal indices $m, m \pm n, m \pm 2n, m \pm 3n$ and so on. For scatterers that are mirror-symmetric, upward and downward coupling must be equal, in the sense that, for example, a mirror-symmetric scatterer of 2nd order rotational symmetry (such as a long rod), T-matrix elements coupling from $m = 1$ modes to $m = -1$ modes will have the same magnitudes as the elements coupling from $m = -1$ to $m = 1$ modes. For chiral scatterers, these T-matrix elements will, in general, be different.

This directly affects the optical torque; the vector spherical wavefunctions are eigenfunctions of the angular momentum operators J^2 and J_z. Essentially, the radial mode index n gives the magnitude of the angular momentum flux, while the azimuthal mode index m gives the z-component of the angular momentum flux. Therefore, the coupling between orders of different m describes the generation of optical torques about the beam axis.

For the case of a rotationally symmetric scatterer, this means that there is no coupling between modes with differing angular momenta about the z-axis [1, 10, 11]. Therefore, it is not possible to exert optical torque on such scatterers except by absorption (or gain) — since the incoming and outgoing angular momenta per photon are the same, the only optical torque can result from a change in the number of photons. In general, the use of absorption for the transfer of optical torque is impractical, due to excessive heating. Therefore, a departure from rotational symmetry is required. This can be either at the macroscopic (the shape of the particle) or microscopic (optical properties of the particle) level.

Birefringent and elongated or flattened particles are simple examples of introducing such asymmetry; notably, such particles were the first to be controllably optically rotated through means other than absorption, for example by Beth in the first measurements of optical torque [12]. Particles with these properties have also been rotated in optical traps [13–16]. As such particles can still be axisymmetric about one axis, rapid calculation of optical forces and torques is still possible [15, 16].

More complex particles have also been fabricated and rotated [17–19], but in these cases, there are few results from computational modelling [20].

As such structures typically possess discrete rotational symmetry, the restrictions on coupling between azimuthal orders can be used to reduce the number of T-matrix elements that need to be calculated. This can greatly reduce the time required. This is also the case for the hybrid methods described above. For a scatterer with pth-order discrete rotational symmetry, it is only necessary to perform calculations for a $1/p$ portion of the entire structure. If, in addition, there is mirror symmetry about the xy plane, the parity of the VSWFs will be preserved. Therefore, an odd-n TE mode will only couple to odd-n TE modes and even-n TM modes. This halves number of non-zero T-matrix elements, and halves the portion of the structure that needs to be modelled.

4. Example: Optical Trapping of a Cube

A simple example illustrating both the relationship between optical torque and symmetry, and the exploitation of particle symmetry for more efficient calculation of optical forces and torques, is the optical trapping of a cube. The cube embodies both of the symmetries — mirror symmetry and discrete rotational symmetry about the normal to the mirror symmetry plane — that typify the ideal optically-driven rotor.

As the cube has 4th-order rotational symmetry, and mirror symmetry with respect to the Cy plane, each incident modes only couples to approximately 1/8 the number of significant scattered modes. Although the column-by-column calculation of the T-matrix still requires the same number of least-squared solutions, each of this is of a smaller system of equations, and much faster. For example, the two wavelengths wide cube used in our example below required 30 minutes for the calculation of the T-matrix on a 32 bit single-processor 3 GHz microcomputer, as compared with 30 hours for an object of the same size lacking the cube's symmetries. Only one octant of the cube was explicitly included in the calculation.

If Figure 1, we show the optical force and torque exerted on a cube with relative refractive index of $1.19 = 1.59/1.34$, and faces 2λ across, where λ is the wavelength in the surrounding medium. Once the T-matrix is calculated, to calculate the optical force and torque at a particular position requires less than 1 second (unless the point is far from the beam focus, in which case, up to 10 seconds or so can be needed).

In Figure 1(a), we see that cubic shapes can be stably trapped axially, while 1(b)–(d) show that optical torque can be generated by such structures. The increased efficiency resulting from the use of orbital angular momentum [5] is clear.

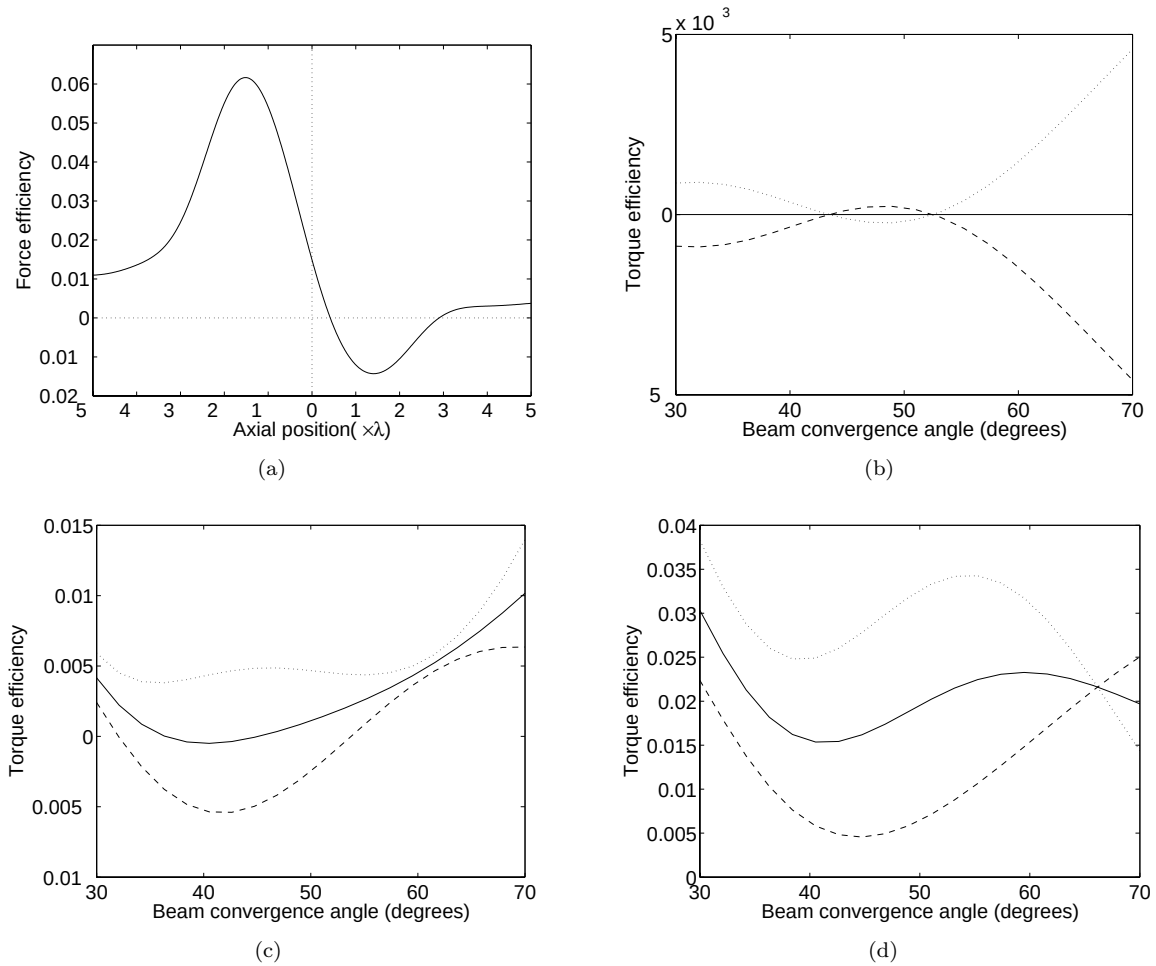

Figure 1: Optical force and torque on a dielectric cube. (a) shows the axial force as a function of position along the beam axis, showing that the cube can be trapped. (b)–(d) show the dependence of the optical torque on the beam convergence angle and the polarisation and orbital angular momentum. In (b), the beam is Gaussian (ie LG_{00}), while in (c) and (d), the beams are LG_{01} and LG_{02} respectively. The solid lines are for plane polarised beams, while dotted and dashed lines are for circularly polarised beams with spin parallel to and antiparallel to the orbital angular momentum.

5. Conclusion

The symmetry properties of a scatterer can be used to dramatically speed the calculation of the scattering properties of a particle. If these are expressed in the form of the T-matrix, this enables rapid and efficient calculation of optical forces and torques. Since typical optically-driven microrotors possess discrete rotational symmetry, they are ideal candidates for this method. In addition, mirror symmetry about a plane can also be used to further reduce the computational burden. Finally, "hybrid" T-matrix methods can be used for particles with geometries or internal structure making them unsuitable for traditional methods of calculating T-matrices.

REFERENCES

1. Waterman, P. C., "Symmetry, unitarity, and geometry in electromagnetic scattering," *Phys. Rev. D*, Vol. 3, 825–839, 1971.
2. Mishchenko, M. I., G. Videen, V. A. Babenko, N. G. Khlebtsov, and T. Wriedt, "T-matrix theory of electromagnetic scattering by particles and its applications: a comprehensive reference database," *J. Quant. Spectrosc. Radiat. Transfer*, Vol. 88, 357–406, 2004.
3. Farsund, Ø. and B. U. Felderhof, "Force, torque, and absorbed energy for a body of arbitrary shape and constitution in an electromagnetic radiation field," *Physica A*, Vol. 227, 108–130, 1996.

4. Crichton, J. H. and P. L. Marston, "The measurable distinction between the spin and orbital angular momenta of electromagnetic radiation," *Elec. J. Differential Equations*, Vol. Conf. 04, 37–50, 2000.
5. Nieminen, T. A., N. R. Heckenberg, and H. Rubinsztein-Dunlop, "Computational modelling of optical tweezers," *Proc. SPIE*, Vol. 5514, 514–523, 2004.
6. Nieminen, T. A., H. Rubinsztein-Dunlop, and N. R. Heckenberg, "Multipole expansion of strongly focussed laser beams," *J. Quant. Spectrosc. Radiat. Transfer*, Vol. 79–80, 1005–1017, 2003.
7. Kahnert, F. M., "Numerical methods in electromagnetic scattering theory," *J. Quant. Spectrosc. Radiat. Transfer*, Vol. 79–80, 775–824, 2003.
8. Nieminen, T. A., H. Rubinsztein-Dunlop, and N. R. Heckenberg, "Calculation of the T-matrix: general considerations and application of the point-matching method," *J. Quant. Spectrosc. Radiat. Transfer*, Vol. 79–80, 1019–1029, 2003.
9. Mackowski, D. W., "Discrete dipole moment method for calculation of the T matrix for nonspherical particles," *J. Opt. Soc. Am. A*, Vol. 19, 881–893, 2002.
10. Mishchenko, M. I., "Light scattering by randomly oriented axially symmetric particles," *J. Opt. Soc. Am. A*, Vol. 8, 871–882, 1991.
11. Nieminen, T. A., "Comment on geometric absorption of electromagnetic angular momentum," C. Konz, G. Benford, *Opt. Commun.*, Vol. 235, 227–229, 2004.
12. Beth, R. A., "Mechanical detection and measurement of the angular momentum of light," *Physical Review*, Vol. 50, 115–125, 1936.
13. Friese, M. E. J., T. A. Nieminen, N. R. Heckenberg, and H. Rubinsztein-Dunlop, "Optical alignment and spinning of laser trapped microscopic particles," *Nature*, Vol. 394, 348–350, 1998.
14. Bonin, K. D., B. Kourmanov, and T. G. Walker, "Light torque nanocontrol, nanomotors and nanorockers," *Opt. Express*, Vol. 10, 984–989, 2002.
15. Bayoudh, S., T. A. Nieminen, N. R. Heckenberg, and H. Rubinsztein-Dunlop, "Orientation of biological cells using plane polarised Gaussian beam optical tweezers," *J. Mod. Opt.*, Vol. 50, No. 10, 1581–1590, 2003.
16. Bishop, A. I., T. A. Nieminen, N. R. Heckenberg, and H. Rubinsztein-Dunlop, "Optical application and measurement of torque on microparticles of isotropic nonabsorbing material," *Phys. Rev. A*, Vol. 68, 033802, 2003.
17. Galajda, P. and P. Ormos, "Complex micromachines produced and driven by light," *Appl. Phys. Lett.*, Vol. 78, 249–251, 2001.
18. Luo, Z.-P., Y.-L. Sun, and K.-N. An, "An optical spin micromotor," *Appl. Phys. Lett.*, Vol. 76, 1779–1781, 2000.
19. Ukita, H. and M. Kanehira, "A shuttlecock optical rotator — its design, fabrication and evaluation for a microfluidic mixer," *IEEE J. Select. Topics Quantum Electron.*, Vol. 8, 111–117, 2002.
20. Collett, W. L., C. A. Ventrice, and S. M. Mahajan, "Electromagnetic wave technique to determine radiation torque on micromachines driven by light," *Appl. Phys. Lett.*, Vol. 82, 2730–2732, 2003.

Optical Microfluidics

J.-P. Delville[1], **R. Wunenburger**[1], **and C. Baroud**[2]

[1]Université Bordeaux, France
[2]LadHyX, France

The development of applications based on microfluidic technology is still hindered by the lack of robust fundamental building blocks that constitute any fluidic system: pumps, valves and mixers for instance. Yet, these building blocks run into the limits of miniaturization and most of the designs used in human-scale flows are either impractical or completely inapplicable to micron-scale flows. On the other hand, while large scale flows are rather insensitive to small leaks, miniaturized fluidic devices become increasingly sensitive to such imperfections. This problem is made worse by the difficulty of micron-scale fabrication, especially when moving parts are involved. An attractive route is optical actuation because light fields are non invasive and dynamically reconfigurable, and solutions have been proposed through the use of optical tweezers to manipulate small particles in flows. By controlling the position and rotation of many particles independently, pumps, valves and particle sorters have been demonstrated in microfluidic channels. The extension of these techniques to multiphase flows is nevertheless difficult because colloidal particles interact with fluid-fluid interfaces.

Here, we propose two types of optical forcing to drive microfluidic two-phase flows or, conversely to answer the requirements enumerated above, namely to block, merge, divide or sort individual droplets flowing in a microchannel. First, we investigate the effect of the optical radiation pressure on fluid interfaces and analyze microfluidic flow regimes in laser-induced jetting, either droplet dripping or continuous transport in laser-sustained liquid columns (Fig. 1). Then, we investigate a dissipative coupling consisting in heating locally an interface between two immiscible fluids to produce thermocapillary stresses along this interface. This effect, known as the optical Marangoni effect, is implemented in adequate microchannel geometry to devise fundamental building blocks for two-phase flows in microfluidic devices (Fig. 2). This allows the creation of contactless optical actuators such as mixers, valves, droplet sorters and switch, droplet dividers or droplet mergers.

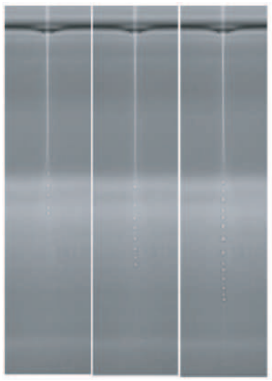

Figure 1: Microfluidic flows driven by the optical radiation pressure, (1) Dynamics of droplet emission during laser-induced jetting (1 fps); (2) Different sort of liquid columns (liquid optical fibres) induced and stabilized by radiation pressure largely beyond the Rayleigh-Plateau instability onset.

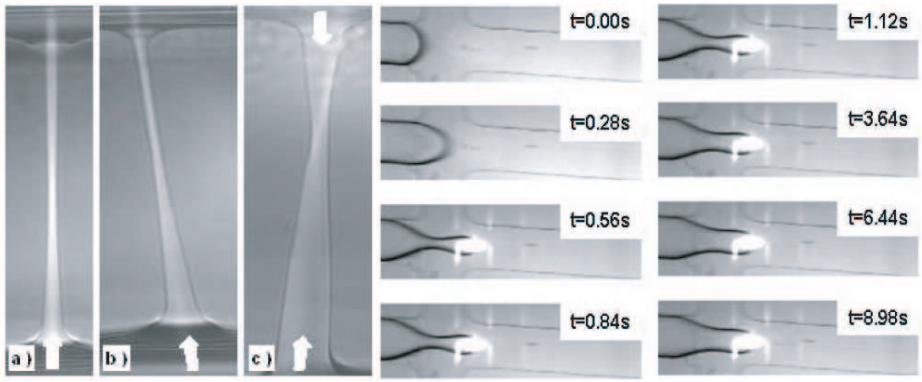

Figure 2: Optical actuation of a water flow in a microchannel, Implementation of an optical valve: the laser pins the interface for several seconds by thermocapillary stresses, producing larger drops of calibrated volume without changing flow rates.

Light-mediated Particle Interactions in a Laser Trap

G. L. Lippi, **S. Barland**, **M. Colombet**, **J. Farmer**, **and R. Kaiser**
Institut Non Linéaire de Nice, France

J.-M. Fournier
Swiss Federal Institute of Technology, Switzerland

Optical manipulation of small objects has been the focus of attention for over three decades and has brought about a revolution in our techical capabilities and in our understanding of the electromagnetic forces acting on different materials ranging from atoms, to dielectric and conductive particles all the way to biological samples. The implications of these developments are so far-ranging that even now we do not foresee their full capabilities.

At first, much of the attention was focussed on the direct forces that are exerted directly on the object by the laser beam used for its control. Recent developments in trapping multiple objects and downscaling the trap's size (and the objects' size as well) open up new questions as to the mutual interactions which take place among the trapped elements. Indeed, when one single coherent beam is used for holding together the sample, the light scattered by each element contributes to the global scattered field which influences all particles. Experimental evidence has already shown that when a sufficiently large number of objects is trapped, the trapping field cannot be considered independently of the scattered components and that the trap is the result of the global superposition of all fields.

We will discuss different aspects of the interaction of multiple particles trapped by a common coherent field. Pairs of spheres [1, 2] and multiplets [3, 4] are known to bind together maintaining preferential distances dictated by the interaction between the scattered and the trapping field. Multiple spheres form structures which depend on the symmetries imposed on the problem.

A such one-dimensional arrangement can be obtained either through the interference of two beams [2] or through a strongly elliptical trap. For this trap geometry the effects of fluctuations are strongly modified in the two directions (parallel and perpendicular to the trapping field). In addition, in the elliptical trap configuration the interaction strength is not constant and can thereby influence the trapping characteristics.

In a two-dimensional arrangements where preferential sites are imposed by the trapping beam [2] the particles mostly sit at the pre-chosen positions but present residual fluctuation-induced motion which is reminiscent of transport problemes. If instead the trap is smooth, states may be found where the particles move quite freely, followed, as the trap power is increased, by "viscous" motion as in a fluid, and terminating in "rigid" structures.

Additional optical interactions may also be induced by cell surfaces, whereby the effectiveness of these contributions depends on the size of the particles, the light polarisation, and in general by the systems parameters. Size considerations will be discussed for downscaling to very small objects.

REFERENCES

1. Burns, M. M., J. M. Fournier, and J. A. Golovchenko, *Phys. Rev. Lett.*, Vol. 63, 1233, 1989.
2. Burns, M. M., J. M. Fournier, and J. A. Golovchenko, *Science*, Vol. 249, 749, 1990.
3. Tartarkova, S. A., A. E. Carruthers, and K. Dholakia, *Phys. Rev. Lett.*, Vol. 89, 283901, 2002.
4. Singer, W., M. Frick, S. Bernet, and M. R. Marte, *J. Opt. Soc. Am.*, Vol. B 20, 1568, 2003.

Non-lorentzian Electromagnetic Resonances

V. A. Markel
University of Pennsylvania, USA

In quantum mechanics, scattering amplitude exhibits resonance behavior if the energy of scattered particles is close to the energy of one of the quasi-stationary states, if such quasi-stationary states exist. For potentials which decay fast enough at infinity, the resonance cross sections, as functions of energy, can be accurately approximated by Lorentzians. A similar phenomenon can be found in electromagnetic scattering. Consider scattering of monochromatic waves with the frequency ω by a homogeneous non-magnetic scatterer of arbitrary shape characterized by the dielectric function $\epsilon(\omega)$. We can define an electromagnetic eigenstate as a solution to $\int_V \hat{G}_0(\omega;\mathbf{r},\mathbf{r}')\mathbf{P}_n(\omega;\mathbf{r}')d^3r' = \xi_n(\omega)\mathbf{P}_n(\omega;\mathbf{r})$. Here V is the volume occupied by the scattering material, $\hat{G}_0(\omega;\mathbf{r},\mathbf{r}')$ is the frequency-domain, dyadic free-space Green's function for the Maxwell's equation which gives electric field at the point $\mathbf{r}$ due to a point dipole oscillating at frequency ω at the point $\mathbf{r}'$, $\mathbf{P}_n(\omega;\mathbf{r})$ is the n-th polarization eigenstate and $\xi_n(\omega)$ is the corresponding eigenvalue (generally, complex). The extinction cross section can be written as a sum over the eigenmodes, i.e., $\sigma_e = \sum_n f_n(\omega)/[z(\omega) - \xi_n(\omega)]$, where $f_n(\omega)$ is the generalized oscillator strength for the n-the eigenmode which has no singularities in the complex plane as a function of ω and $z(\omega)$ is the spectral variable defined by $z(\omega) = (4\pi/3)[\epsilon(\omega)+2]/[\epsilon(\omega)-1]$ [1]. Electromagnetic resonances take place when the denominator in the above equation is in some sense small. However, the imaginary part of the denominator can not vanish due to energy conservation considerations. Therefore, we define resonance frequencies ω_n as solutions to $\mathrm{Re}[z(\omega_n) - \xi_n(\omega_n)] = 0$. If ω is close to one of the resonance frequencies ω_n, and if $\xi_n(\omega)$ and $f_n(\omega)$ change slowly in the vicinity of ω_n, one can make the quasi-particle pole approximation and write $\sigma_e \approx [f_n(\omega_n)/z'(\omega_n)]/[\omega - \omega_n + i\gamma_n]$, where $\gamma_n = \mathrm{Im}[z(\omega_n) - \xi(\omega_n)]/z'(\omega_n)$ and prime denotes differentiation. This resonance has the typical Lorentzian structure with the lifetime $\tau_n = 1/\gamma_n$ which is determined by the sum of Ohmic ($\mathrm{Im}[z(\omega_n)]$) and radiative ($-\mathrm{Im}[\xi(\omega_n)]$) losses.

In scatterers which are small compared to the external wavelength, the quasi-particle pole approximation is, typically, quite accurate. This is due to the fact that, within the quasistatics, the real parts of $\xi_n(\omega)$ are ω-independent an satisfy $-8\pi/3 < \mathrm{Re}\xi_n < 4\pi/3$ [2]. In extended systems these statements are, generally, not valid. In particular, in a long periodic chain of nanospheres, real parts of eigenvalues ξ_n diverge logarithmically near certain frequencies which are determined from the synchronism condition [3]. This divergence leads to electromagnetic resonances which are essentially non-Lorentzian. In particular, their width is determined not by relaxation but by the range of frequencies in which the equation $\mathrm{Re}[z(\omega) - \xi_n(\omega)] = 0$ is approximately satisfied. It was shown that these resonances are super-exponentially narrow with the width being proportional to the factor $\exp[-C(h/a)^3]$, where C is a numerical constant of the order of unity, h is the period of the chain and a is the nanosphere radius [4]. The divergence of eigenvalues can also lead to narrow spectral holes which were already reported in [3]. Recent advances in nanofabrication have reinvigorated interest in one-dimensional chains of nanoparticles. A dramatic narrowing of spectral lines and unusual properties electromagnetic resonances were found numerically in chains of large but finite length in [5]. The origin and properties of these resonances in infinite chains were discussed theoretically in [4]. Theoretical treatment of finite chains was recently given in [6].

REFERENCES

1. Markel, V. A. and E. Y. Poliakov, *Phil. Mag.*, Vol. 76, 895, 1997.
2. Markel, V. A., V. N. Pustovit, S. V. Karpov, A. V. Obuschenko, V. S. Gerasimov, and I. L. Isaev, *Phys. Rev. B*, Vol. 70, 054202, 2004.
3. Markel, V. A., *J. Mod. Opt.*, Vol. 40, 2281, 1993.
4. Markel, V. A., *J. Phys. B*, Vol. 38, L115, 2005.
5. Zou, S., N. Janel, and G. C. Schatz, *J. Chem. Phys.*, Vol. 120, 10871, 2004.
6. Citrin, D. S., *Nano Letters*, Vol. 5, 985, 2005.

Exact Calculations of Optical Forces and Optical Binding in Single and Multiple Beam Optical Traps

O. Moine and B. Stout
Université Paul Cézanne Aix-Marseille III et Université de Provence, France

We present essentially exact multi-pole multi-scattering techniques for carrying out optical force calculations in a wide variety of optical trapping situations involving either isolated particles or collections of simultaneously trapped particles.

We illustrate that our exact techniques [1] can quite readily be applied to a variety of trapping situations and particle types for which popular approximate techniques (Rayleigh, geometric optics, Born approx. etc.) are either inapplicable or exceedingly difficult to carry out.

In particular, we highlight the use of our techniques to investigate the intriguing optical binding and optical "crystallization" observed in multiple-beam interferential optical traps [2–4].

We also rapidly illustrate applications of our techniques to the widely employed single-beam optical traps known as optical tweezers. In particular, we discuss the techniques which we have developed in order to model the extremely tightly focused beams which are essential to standard optical tweezers.

REFERENCES

1. Moine, O. and B. Stout, "Optical force calculations in arbitrary beams by use of the vector addition theorem," *JOSA B*, Vol. 22, No. 8, 1620–1631, 2005.
2. Burns, M., J. M. Fournier, and J. A. Golovchenko, "Optical Matter: crystallization and binding in intense optical fields," *Science*, Vol. 249, 713–828, 1990.
3. Burns, M. M, J. M. Fournier, and J. A Golovchenko, "Optical binding," *Phys. Rev. Lett.*, Vol. 63, 1233–1236, 1989.
4. "Optical binding between dielectric particles," *Opt. Express*, Vol. 12, No. 12, 2746–2753, 2004.

Shaping Electromagnetic Fields for Optical Trapping and Binding

J.-M. Fournier, **P. Jacquot**, **J. Rohner**, **and R.-P. Salathé**
Imaging and Applied Optics Institute, Switzerland

Optical traps can be built simply from constructive and destructive interference of two or more coherent light beams. For example, interference of several identical plane waves distributed with an n-fold symmetry lead to periodic or aperiodic arrays of traps [1]. Figure 1 displays such a set of traps. Interference between an intense electromagnetic field impinging on mesoscopic particles and fields scattered by such particles generate ensembles of self distributed traps [2]. This leads to assemblies of the type of the one shown in Figure 2. Other kinds of interference made with two or more beams presenting a variety of complex amplitude distributions lead to atypical intensity landscapes presenting endless configuration possibilities for trap potentials [3]. The design of various trap shapes can then be manipulated at will through such interference, in order to control trap strength or also to command optical forces which channel polarizable dielectric particles. Besides, one can simply take advantage of free space wave propagation to form interference by illuminating a diffractive pattern with a plane wave or with a spherical wave.

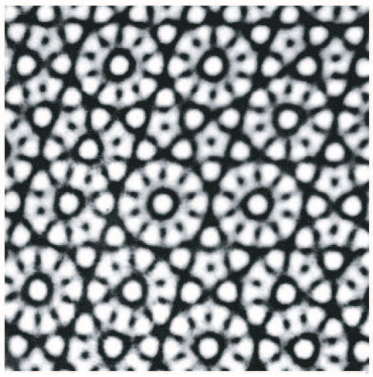

Figure 1: Five-fold symmetry array of optical traps.

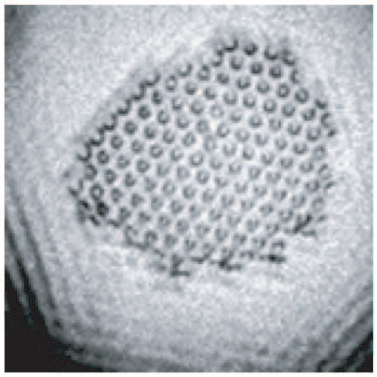

Figure 2: Dielectric particles assembled with gradient and binding forces.

The scope of this paper is to review and discuss several uncommon optical trap designs, such as those using Talbot imaging, a periodic diffractive structure, speckle patterns, or multiple beam interference. Experimental results emphasize the capability of the Talbot effect to generate three-dimensional optical lattices with the advantage of creating stiff traps with strong gradient forces. Several schemes of self-organization representing interesting means for trapping will also be described and discussed.

Mechanisms involved in those trapping procedures do not require the use of bulky high numerical aperture optics and are under test to produce new regimes of optical trapping. Most of the investigated designs account for the possibility of creating large arrays of traps.

REFERENCES

1. Burns, M. M., J.-M. Fournier, and J. A. Golovchenko, "Optical matter, crystallization and binding in intense optical fields," *Science*, Vol. 249, 749–754, 1990.
2. Burns, M. M., J.-M. Fournier, and J. A. Golovchenko, "Optical binding," *Phys. Rev. Lett.*, Vol. 63, 1233–1236, 1989.
3. Fournier, J.-M., J. Rohner, P. Jacquot, R. Johann, S. Mias, and R. P. Salathé, "Assembling mesoscopic particles by various optical fields," *Trapping and Optical Micromanipulation II, SPIE Proc.*, Vol. 5514, 2005.

Theory and Modeling of Optical Forces within a Collection of Mie Scatterers

T. M. Grzegorczyk, B. A. Kemp, and J. A. Kong
Massachusetts Institute of Technology, USA

Optical binding and trapping have been experimentally verified on dielectric particles by various groups [1–4, to name only a few]. The corresponding theoretical analysis, however, still needs to be developed beyond the simple approximations of Rayleigh scattering or couple of Mie particles. In this work, we present an exact method to compute the optical forces within a system of multiple Mie particles. For the sake of simplicity, the particles are taken to be lossless dielectric cylinders, which is not a severe limitation per se since apart from the depolarization effects, most of the phenomena observed in two-dimensions can be generalized to three-dimensions.

The optical forces are computed from the Maxwell stress tensor, which therefore requires the knowledge of the scattered field from the collection of particles. The latter is computed from the Mie theory for cylinders and the Foldy-Lax multiple scattering equations, which take into account all the interactions between the particles. Hence, apart from the assumption of real permittivity, the method does not make any approximation on the size of the particles or their number in the collection.

In order to conform to the experimental setup, the system of particles is excited by three incident beams, forming an hexagonal interference pattern. For the sake of illustration, we present results for a collection of 20 particles initially randomly positioned in the interference field, like shown in Fig. 1. The forces on each particle is computed and their positions are updated accordingly. At the next time step, the forces are computed anew with the new positions, and the process is reiterated until convergence has been obtained, shown in Fig. 2. It can be seen that for the particle size considered, a gradient force is exerted on the particle which tends to align them with the high eld intensity regions. However, binding forces between the particles tend to disrupt this regular pattern and it is seen that the nal positions of some particles (typically toward the edge of the collection) is shifted from the expected positions. We believe that it is the rst time that this phenomenon, known in experimental situations, is shown by an analytical modeling.

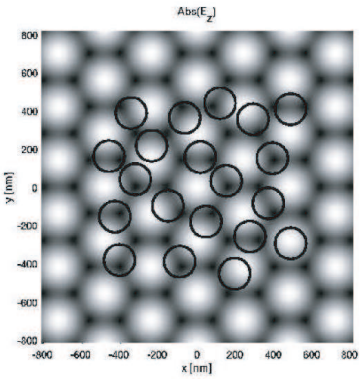

Figure 1: Initial positions of 20 particles in an interference field.

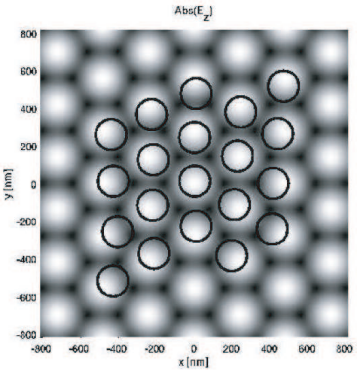

Figure 2: Final positions of 20 particles due to optical forces.

REFERENCES

1. Ashkin, A., "Acceleration and trapping of particles by radiation pressure," *Phys. Rev. Lett.*, Vol. 24, 156–159, 20 January 1970.
2. Burns, M. M., J.-M. Fournier, and J. A. Golovchenko, "Optical binding," *Phys. Rev. Lett.*, Vol. 63, No. 12, 1233–1236, 1989.
3. Zemánek, P., A. Jonáš, L. Šrámek, and M. Liška, "Optical trapping of nanoparticles and microparticles by a gaussian standing wave," *Optics Letters*, Vol. 24, 1448–1450, 1 November 1999.
4. Fournier, J.-M., J. Rohner, P. Jacquot, R. Johann, S. Mias, and R. Salathé, "Assembling mesoscopic particles by various optical schemes," *Proceedings of SPIE*, 2005.